A Study of Sparse Detector Designs with Interpolation for Multi-Slice Spiral CT

Darius Coelho and Klaus Mueller

***Abstract*—In multi-slice spiral CT, z-sampling has a great effect on image quality, dose and speed. In our work, we explore using sparse detectors of various designs in multi-slice spiral CT. These designs have fewer detector elements as compared to a regular detector. Or alternatively, they have the same number of detectors but provide more axial coverage for greater scanning speed of longer objects. The sparser detector elements also affect the reconstruction in a similar manner as z-sampling does. To account for the missing detector elements we interpolate the acquired data to simulate a full detector. We apply both bilinear interpolation and directional interpolation and compare them. We also report the quality of the reconstruction, the amount of dose and scan speed for each detector pattern.**

I. Introduction

The multi-slice spiral CT systems used today have brought about considerable improvements in terms of scan speed and transverse resolution as compared to the initial single slice spiral CT systems. One of the challenges in multi-slice spiral CT is how to achieve efficient z-sampling using a multi-row detector. The pitch in helical CT has a major impact on z-sampling, and a detailed explanation about its affect on multi-slice spiral CT is provided by Goldman [1]. To this end researchers have conducted many studies related to pitch and angular sampling for spiral CT. Increasing the pitch can improve the scan speed but at the same time reduce the image quality of the reconstructions.

One method that has been used extensively to improve the image quality is interpolation. Sophisticated interpolation algorithms such as MUSCOT by Taguchi and Aradate [2] and the Adaptive Axis Interpolator, AAI, by Schaller et al. [3] have been described more than a decade ago. MUSCOT is fairly efficient, while AAI is somewhat more involved. More recently, Bertram et al. [4] and Li et al. [5] use interpolation to compute the missing projections in the angular domain.

In this paper, we describe a variety of new detector layouts for spiral CT. We propose a reduction in the number of detector elements and layout these detector elements in three different patterns. These detectors are elongated versions of current detectors and thereby affect the z-sampling. The elongated detector patterns also allow us to scan a larger area in the same amount of time thus allowing faster scans. To maintain the image quality of the reconstruction we interpolate the data at the sites of the missing detector elements. We test two interpolation schemes: 1) bilinear interpolation which is one of the most widely used interpolation methods 2) directional interpolation which interpolates along edges or in the direction of the gradient as explained by Tam et al. [6]. Finally we evaluate the performance of these detector designs and interpolation schemes.

Paper submitted on May 2, 2015. This work was supported by the MSIP, Korea, under the "ICT Consilience Creative Program" (IITP-2015-R0346-15-1007).

Darius Coelho and Klaus Mueller are with the Visual Analytics and Imaging Lab, Computer Science Department, Stony Brook University and SUNY Korea (e-mail: {dcoelho, mueller}@cs.stonybrook.edu).

II. Approach

As mentioned in the introduction we propose three different layouts as shown in Fig. 1(second row). In the layout of Detector 1 we remove every alternate detector row from the original detector thus using half the number of detector elements as compared to the original detector. This is somewhat similar to decreasing the z-sampling. In the second layout for Detector 2, we use a checkerboard pattern which is equivalent to a hexagonal grid and uses the same number of detector elements as Detector 1. This layout collects samples more uniformly. In the third and final layout for Detector 3 we create a sparse grid of detector elements by removing every alternate detector row and column from the regular detector thus using 25% of the detector elements as compared to a regular detector.

The design of spiral scanning path is interesting for Detectors 1 and 3 since both of them would be twice as long as a regular detector if we kept the same number of rows. We now have a large gap between the detector rows thereby reducing z-resolution which we overcome via interpolation. But to further improve the quality of the interpolation we select a spiral scanning pitch such that projections 180° apart interleave rather than duplicate. Thus we can calculate the amount of table movement as $2n \times d$. Here d is the height of a detector element and n is an odd number less than the number of detector rows. Also note that for Detector 2 the missing elements on the detector interleave with the elements from the complementary projection without the requirement of a detector shift.

To account for the missing detector elements in our detector patterns we interpolate the values at their positions. We perform the interpolation on every projection we acquire after which we perform the reconstruction using these projections. We have applied both bilinear interpolation and directional interpolation algorithms on our detectors. We interpolate the intensity as follows:

$$I(x,y) = \frac{\sum I(x+i, y+j).w(x+i, y+j)}{\sum w(x+i, y+j)}$$

where $(i,j) = (-1,-1),(0,-1),(1,-1),(-1,0),(1,0)(-1,1),(0,1),(1,1)$

Here $I(x,y)$ is the intensity value of the detector element at position (x,y) and $w(x,y)$ is a weighting factor. For bilinear interpolation the weights are set to 1. But for directional interpolation the weights are computed based on the gradient of the neighboring pixels at every interpolation point. By giving a higher weighting factor in the direction of the gradient we can emphasize prominent structures in the projection.

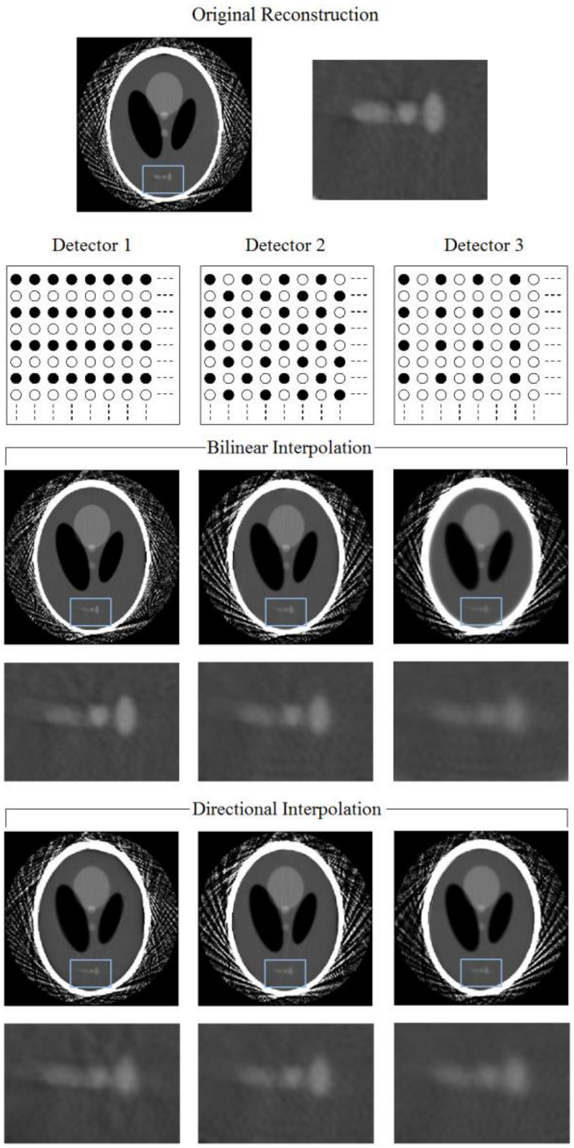

Fig. 1. Reconstruction of the 3D Shepp-Logan head phantom shown for slice Z = -0.25. The top row is the gold standard reconstruction using a 16 row complete detector with the tumor zooms. The second row shows the different detector layouts. The next four rows show reconstruction results, along with a zoomed in view of the tumors, using bilinear interpolation and directional interpolation with our detector designs.

III. Results And Discussion

We test our approach with the 3D Shepp-Logan Phantom. A slice of the reconstructions is shown in Fig. 1. We chose this slice as there are three tumors located close to each other and we can see the effect the interpolation and detector pattern has on their reconstruction. The zoomed in views of the tumors for each case are shown in Fig 1 as well.

We observe that for all cases we can still see all the structures that are present in the original reconstruction. We can also differentiate between the three tumors highlighted in the images. But we do observe some artifacts in the reconstructions for Detectors 2 and 3. We also observe that among our detector designs, Detector 1 performs quite well, Detector 2 introduces some blurring and in Detector 3's reconstruction the blurring is quite obvious. Comparing the interpolation methods we see that for the layout of Detector 1 bilinear interpolation performs better than directional interpolation. This is clearly visible when we compare the zoomed in views of the tumors. For Detector 2 both bilinear interpolation and directional interpolation provide similar quality reconstructions, there isn't much difference in image quality between both images. Finally for Detector 3 we see that directional interpolation outperforms the bilinear interpolation. In the zoomed in view we can see that the tumors are just beginning to merge. Thus we conclude that as the detectors become more sparse directional interpolation is advantageous.

The quantitative evaluation is shown in Table 1. It shows the quality, amount of dose and scan time for each of the detectors as compared to a denser detector with the same number of elements. To quantitatively measure the image quality we computed the correlation coefficient of each reconstruction with the reconstruction of a regular 16×138 element detector. We report the speed as a ratio of the coverage per rotation of our detectors versus regular sized detectors with the same number of rows. The reduced pitch required to interleave complementary projections is also factored in.

Detector Design	**Detector 1**	**Detector 2**	**Detector 3**
Quality (CC)	0.989 (Bilinear)	0.978 (Directional)	0.958 (Directional)
Speed (relative to regular detector)	1.545	1	1.545

Table 1. Performance analysis of our detectors in terms of image quality (the better interpolation method was chosen for each detector) and scan speed.

IV. Conclusion

In this work we studied three sparse detector layouts and two interpolation schemes for multi-slice spiral CT reconstruction. Two of the designs offer improved scan speed. Our results ~~have~~ show that even though we use sparse detectors, interpolation still provides us with feasible reconstructions. Our evaluation provides us with the advantages and disadvantages of each detector and interpolation methods and thus allows us to choose a suitable detector depending on the desired image quality and scan speed. In future work we plan to conduct studies with real data.

References

[1] Goldman, L. W. "Principles of CT: multislice CT." *Journal of nuclear medicine technology* 36, no. 2 (2008): 57-68.

[2] K. Taguchi and H. Aradate, "Algorithm for image reconstruction in multi-slice helical CT," *Medical Physics*, 25(4):550-561, 1998.

[3] Schaller, S., Flohr, T., Klingenbeck, K., Krause, J., Fuchs, T., & Kalender, W. A. (2000). Spiral interpolation algorithm for multislice spiral CT. I. Theory. *Medical Imaging, IEEE Transactions on*, 19(9), 822-834.

[4] Bertram, M., Wiegert, J., Schafer, D., Aach, T., & Rose, G. (2009). Directional view interpolation for compensation of sparse angular sampling in cone-beam CT. *Medical Imaging, IEEE Transactions on*, 28(7), 1011-1022.

[5] Li, Y., Chen, Y., Hu, Y., Oukili, A., Luo, L., Chen, W., & Toumoulin, C. (2012). Strategy of computed tomography sinogram inpainting based on sinusoid-like curve decomposition and eigenvector-guided interpolation. *JOSA A*, 29(1), 153-163.

[6] Tam, W. S., Kok, C. W., & Siu, W. C. (2010). Modified edge-directed interpolation for images. *Journal of Electronic imaging*, 19(1), 013011-013011.